JOC The Journal of Organic Chemistry

Article

pubs.acs.org/joc

Reactivity of Endohedral Metallofullerene $La_2@C_{80}$ in Nucleophilic and Electrophilic Attacks: Vibronic Coupling Density Approach

Naoki Haruta,[†] Tohru Sato,*[,†,‡] and Kazuyoshi Tanaka[†]

[†]Department of Molecular Engineering, Graduate School of Engineering, [‡]Unit of Elements Strategy Initiative for Catalysts & Batteries, Kyoto University, Nishikyo-ku, Kyoto 615-8510, Japan

Supporting Information

ABSTRACT: The regioselectivities of $La_2@C_{80}$ in thermal nucleophilic and electrophilic attacks were theoretically investigated using vibronic coupling density (VCD) analysis. Nucleophilic and electrophilic cycloadditions to $La_2@C_{80}$ were experimentally reported to yield [6,6] and [6,5] adducts, respectively, as major products. VCD analysis provided a clear explanation for these experimental results. For nucleophilic reactions, it was found that the reactive [6,6] bonds did not have a large lowest unoccupied molecular orbital (LUMO) density and Fukui function but a large potential derivative with respect to a reaction mode. The VCD illustrates the origin of the interaction between the electronic and vibrational states. On the other hand, conventional reactivity indices such as frontier orbital density take only the electronic state into account. The result suggested that the stabilization due to vibronic couplings plays an important role in the regioselectivity of nucleophilic cycloadditions. The VCD with respect to the effective mode could provide a picture of the functional groups, which are the double bonds of ethylene moieties. VCD analysis with respect to hypothetical localized modes enabled the quantitative prediction of regioselectivities.

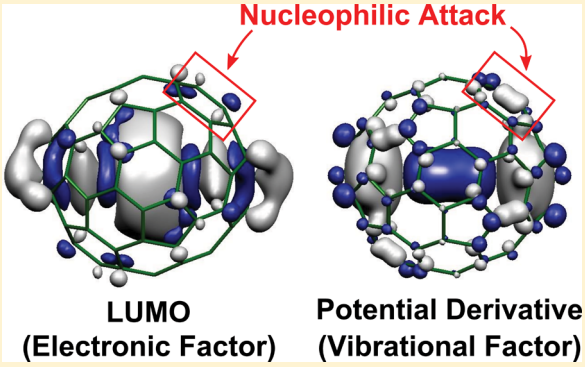

1. INTRODUCTION

Endohedral metallofullerenes, which consist of a carbon spherical cage with encapsulated metal atoms, have received much attention[1−6] since they were first reported.[7] The electronic states of the outer carbon cage can be varied by changing the encapsulated atoms. Endohedral metallofullerenes are expected to have applications in field-effect transistors,[8] photovoltaics,[9] and drug delivery materials.[10]

$La_2@C_{80}$ is an abundant endohedral metallofullerene; therefore, its properties and reactivity have been investigated in detail, both experimentally and theoretically.[2,3] It consists of a C_{80} cage with I_h symmetry and two encapsulated lanthanum atoms. $La_2@C_{80}$ has various isomers with symmetries lower than I_h, depending on the La_2 configuration (examples are shown in Figure 1). Theoretical results regarding the most stable isomer are controversial: Shimotani et al.[11] reported that the D_{2h} isomer is the most stable, whereas Zhang et al.[12] found the D_{3d} isomer to be the most stable. The thermal rotation of the La_2 molecule inside $La_2@C_{80}$ at room temperature has been experimentally observed.[2,3]

The carbon bonds in $La_2@C_{80}$ can be classified into two types: [6,6] and [6,5] bonds. The [6,6] bonds are shared by two adjacent six-membered rings, whereas the [6,5] bonds are shared by six- and five-membered rings. According to the experimental work of Yamada et al.,[13,14] the nucleophilic cycloaddition of *N*-triphenylmethyl azomethine ylide to $La_2@C_{80}$ yields two types of isomers with a ratio of 4:1. The major product is a [6,6] monoadduct, whereas the minor one is a [6,5] monoadduct. In addition, Yamada et al.[15] reported the electrophilic cycloaddition of tetracyanoethylene oxide to $La_2@C_{80}$, which yields only a [6,5] monoadduct. Recently, Takano et al.[16] reported the reaction of $La_2@C_{80}$, azomethine ylide (AY), and 11,11,12,12-tetracyano-9,10-anthra-*p*-quinodimethane (TCAQ-CHO), with the latter known to be a strong electron acceptor. In this reaction, two types of the [6,5] monoadduct of $La_2@C_{80}$ and AY connected to TCAQ-CHO were obtained. The structures of a few products from these cycloadditions were observed at low temperatures using X-ray single-crystal diffraction.[13−15] In addition, several photochemical reactions to $La_2@C_{80}$ have been reported.[17−20] Recently, Garcia-Borràs et al.[21] calculated the activation energies for thermal cycloadditions of butadiene to endohedral metallofullerenes including $La_2@C_{80}$ using the frozen cage model. According to this computational study, the major product for the cycloaddition of butadiene to $La_2@C_{80}$ is a [6,5] monoadduct.

Frontier orbital theory,[22,23] Mulliken population analysis,[24] and π-orbital axis vector (POAV) analysis[25] have frequently been used to predict the reactivity of fullerenes. These theories focus on electronic states or static structural strains. Recently, we proposed the concept of vibronic (electron-vibration) coupling density (VCD) for a reaction mode.[26,27] With VCD

Received: September 26, 2014
Published: November 12, 2014

   dx.doi.org/10.1021/jo502208t | *J. Org. Chem.* 2015, 80, 141−147

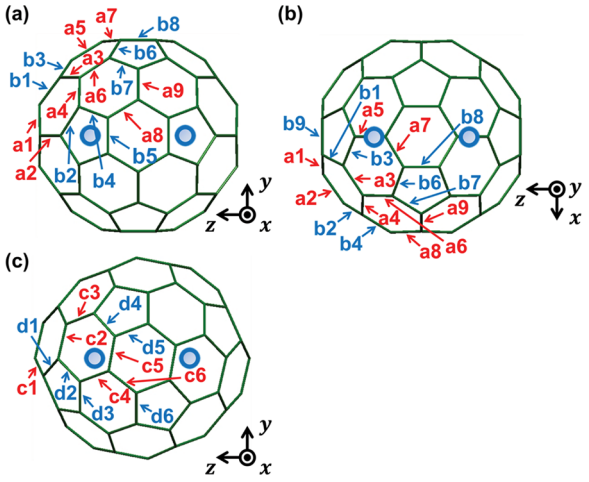

Figure 1. Structures of $La_2@C_{80}$ isomers with carbon bonds labeled: (a, b) D_{2h} isomer from different perspectives and (c) D_{3d} isomer. Red labels indicate [6,6] bonds shared by adjacent hexagonal rings. Blue labels indicate [6,5] bonds shared by hexagonal and pentagonal rings. Schlegel diagrams are also shown in the Supporting Information (Figures S1).

analysis, the reactivities for the Diels–Alder reactions of C_{60},[28−30] C_{70},[31] and styrene[32] and electrophilic addition to naphthalene[27] were successfully elucidated. In the Diels–Alder reaction, C_{60} acts as a dienophile like ethylene, and the VCD for its effective mode also has a similar distribution to that of ethylene.[28] In other words, C_{60} bears ethylene moieties as functional groups from the perspective of VCD. The relative yields of C_{60} bisadduct isomers and the regioselectivities of the multiple adducts up to the hexakisadduct were also predicted.[29,30] The regioselectivity can be quantitatively predicted by estimating vibronic coupling constants (VCCs) with respect to hypothetical localized modes. A picture of the functional group can also be extracted by employing VCD analysis with respect to an effective mode. Regioselectivity can be discussed on the basis of vibronic couplings by considering both the effective and localized stretching modes. VCD analysis is also effective in clarifying the difference between the reactivities under thermal and mechanochemical conditions.[33] In this study, we applied these reactivity indices for nucleophilic and electrophilic reactions of the endohedral metallofullerene $La_2@C_{80}$ to elucidate the role of vibronic couplings in cycloadditions to $La_2@C_{80}$.

2. THEORY

For a reactant, e.g., a metallofullerene, the VCC V_α of a charge-transfer (ionic) electronic state Ψ_{CT} with respect to a vibrational mode α is defined as

$$V_\alpha = \int \Psi_{CT}^{*} \left(\frac{\partial \hat{H}}{\partial Q_\alpha} \right)_{\mathbf{R}_0} \Psi_{CT} \, d\tau \tag{1}$$

where $\hat{H}$ is the molecular Hamiltonian, Q_α denotes a vibrational coordinate of mode α, τ stands for all spatial and spin coordinates of electrons, and $\mathbf{R}_0$ is the reference nuclear configuration (molecular geometry before the charge transfer). V_α can be expressed in the density form using the VCD η_α:[26,27]

$$V_\alpha = \int \eta_\alpha(\mathbf{r}) d^3\mathbf{r} \tag{2}$$

where $\mathbf{r}$ stands for the spatial coordinates. The VCD η_α is defined as

$$\eta_\alpha(\mathbf{r}) = \Delta\rho(\mathbf{r}) \times \upsilon_\alpha(\mathbf{r}) \tag{3}$$

where $\Delta\rho$ denotes the electron density difference between the neutral and charge-transfer states at the geometry $\mathbf{R}_0$, and υ_α is the derivative of the nuclear-electronic potentials acting on a single electron with respect to Q_α at $\mathbf{R}_0$. The derivation of eqs 2 and 3 is described in the Supporting Information. $\Delta\rho$ is equal to the Fukui function[34] within the finite difference approximation. The VCD illustrates the origin of vibronic coupling on the basis of electronic and vibrational structures.

The vibrational mode α in the definition of VCD is not only a normal mode but also an effective[27] or localized mode.[31] The effective mode in the charge-transfer state is defined by the sum of all normal modes weighted by the VCCs with respect to the normal modes. Using the Hellmann–Feynman theorem,[35,36] it can be shown that it is equal to the steepest descent direction of the adiabatic potential in the charge-transfer state. The effective mode can therefore be regarded as a reaction mode. The VCD distribution for the effective mode visualizes the origin of vibronic coupling in the initial stage of a reaction. The localized mode is used as a hypothetical reaction mode to estimate the reactivity of each bond quantitatively.

The reagent is stabilized owing to vibronic couplings after charge transfer. In this work, the direction of the effective mode is taken such that its VCC is negative. This is the direction of a deformation such that the system is stabilized. On the other hand, the direction of the localized mode is taken such that the corresponding bond is elongated by a positive displacement.

3. COMPUTATIONAL METHOD

A neutral $La_2@C_{80}$ with D_{2h}/D_{3d} symmetry was optimized to obtain its reference nuclear configuration $\mathbf{R}_0$. Symmetry constraints were used because of the pseudodegeneracy of the neutral $La_2@C_{80}$ states with D_{2h} and D_{3d} symmetries.[11,12] After optimization, vibrational analyses of the D_{2h} and D_{3d} structures were performed to obtain their frequencies and normal modes. The forces acting on the nuclei of the D_{2h}/D_{3d} anionic and cationic states were subsequently calculated. The anionic and cationic states can be regarded as the charge-transfer states in nucleophilic and electrophilic reactions with $La_2@C_{80}$. In these calculations, density functional theory was used with the VWN+BP86 functional[37−39] and the TZ2P and TZP all-electron basis sets[40] for carbon and lanthanum atoms, respectively. The relativistic effect was taken into consideration within the scalar zeroth-order regular approximation (ZORA).[41] Calculations were done using the Amsterdam Density Functional (ADF) package version 2012.01d.[42−44] For the open-shell unrestricted calculations, spin contamination was confirmed to be sufficiently small ($0.75 < \langle S^2 \rangle < 0.753$). The obtained electronic and vibrational structures were used to calculate the VCCs and VCDs for the effective and localized modes at all types of carbon bonds in the charge-transfer states. The computed forces were used to calculate the VCCs following the Hellmann–Feynman theorem.[35,36] The calculations of the VCCs and VCDs were performed using in-house codes.

4. RESULTS AND DISCUSSION

4.1. Nucleophilic Attack on $La_2@C_{80}$. Figure 2 shows the electron density differences $\Delta\rho$ between the neutral $La_2@C_{80}$ isomers and their anions. $\Delta\rho$ consists mainly of the lowest unoccupied molecular orbital (LUMO) densities of the $La_2@C_{80}$ isomers. Because $\Delta\rho$ has large distributions on lanthanum atoms, the isosurface values in Figure 2 were sufficiently reduced for the distributions to be clearly shown on the C_{80} cage. As shown in Figure 2, except for the region inside the

dx.doi.org/10.1021/jo502208t | J. Org. Chem. 2015, 80, 141−147

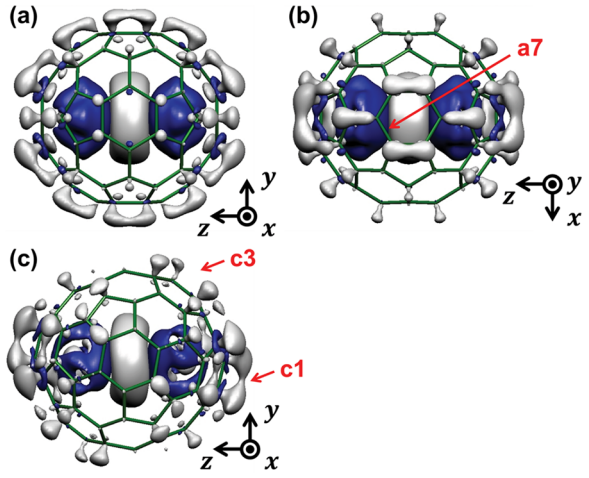

Figure 2. Electron density differences $\Delta\rho$ between neutral and anionic states of isolated $La_2@C_{80}$ isomers: (a, b) D_{2h} isomers from different perspectives and (c) D_{3d} isomer. Isosurface values are 5.5×10^{-4} a.u. Blue surfaces show negative regions (electron decrease), and gray surfaces show positive regions (electron increase). The c3 and a7 bonds have small distributions. Vibronic coupling calculations, however, indicate that the c3 and a7 bonds are the first and second reactive sites, respectively (see Figure 6). On the other hand, the c1 bonds are not reactive sites regardless of the large $\Delta\rho$.

cage, $\Delta\rho$ has the largest distributions around the c1 bonds. On the other hand, the c3 and a7 bonds have small distributions because the corresponding LUMOs are small and antibonding.

Figures 3 and 4 show the effective modes s for the $La_2@C_{80}$ anions and the corresponding potential derivatives υ_s,

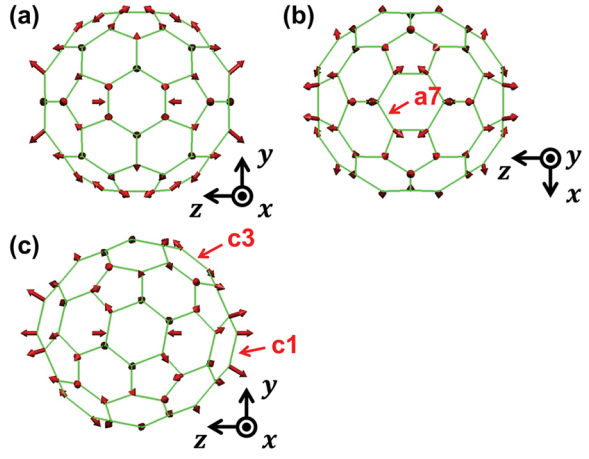

Figure 3. Effective vibrational vectors s of isolated $La_2@C_{80}$ anions: (a, b) D_{2h} isomers from different perspectives and (c) D_{3d} isomer. The c3 and a7 bonds are elongated by the effective modes. In contrast, the cage sites around the c1 bonds are bent and moved outward.

respectively. These indicate the nuclear motions induced by charge transfer. As shown in Figure 4, υ_s has characteristic positive distributions on a few [6,6] bonds such as c3 and a7 bonds, which are elongated by bond stretching vibrations (Figure 3) that facilitate nucleophilic cycloadditions. The c3 bonds have larger positive distributions than that of the a7 bonds. On the other hand, the sites around the c1 bonds do not have such on-bond distributions of υ_s because these sites are

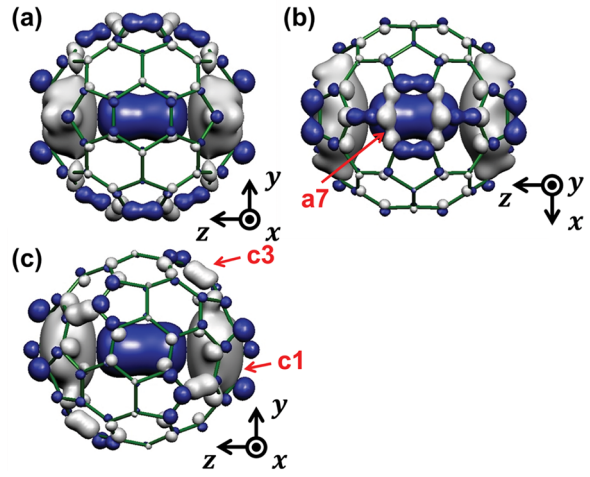

Figure 4. Potential derivatives υ_s for effective modes s of isolated $La_2@C_{80}$ anions: (a, b) D_{2h} isomers from different perspectives and (c) D_{3d} isomer. Isosurface values are 3.0×10^{-3} a.u. Blue surfaces show negative regions, and gray surfaces show positive regions. A large positive distribution on a bond indicates that the bond is easily elongated by the approach of a nucleophile. The c3 and a7 bonds have the largest and second largest positive distributions, respectively, whereas the c1 bonds do not have such distributions.

moved by bending vibrations and not by bond stretching vibrations.

Figure 5 shows the η_s of $La_2@C_{80}$ anions for the effective modes as well as that of the ethylene anion for comparison.

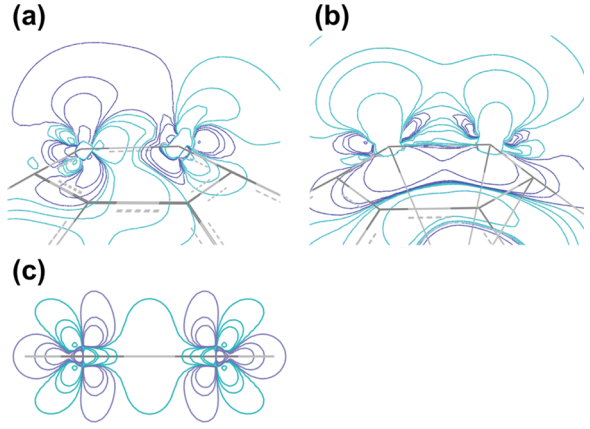

Figure 5. Vibronic coupling densities (VCDs) η_s of isolated $La_2@C_{80}$ anions for the effective modes: (a) c3 bond and (b) c1 bond. (c) η_s of ethylene anion for the effective mode. The VCD at the c3 bond is similar to that of the ethylene anion. On the other hand, the VCD at the c1 bond, which has a large $\Delta\rho$, is completely different from that of the ethylene anion.

Although the symmetries around the c3 and c1 bonds are lower than that of ethylene, the corresponding η_s distributions (Figure 5a,b, respectively) can be recognized. This is because the effective mode consists of bond stretching modes on c3 bonds, which are close to the effective mode for the ethylene anion. In our previous studies on C_{60},[28] C_{60} derivatives,[29,30] and C_{70},[31] it was found that their reactive sites bear functional groups with ethylene-like distributions of η_s. The c3 bonds can therefore be regarded as the reactive sites. Because these bonds do not have large $\Delta\rho$, υ_s is found to be important in nucleophilic cycloadditions. Thus, this result is different from those of

dx.doi.org/10.1021/jo502208t | J. Org. Chem. 2015, 80, 141−147

frontier orbital theory, Mulliken population analysis, and POAV analysis, as shown in the Supporting Information (Figures S4, S6, and S7, respectively). In contrast to the c3 bonds, ethylene moieties cannot be found at the c1 bonds because the effective mode consists of bending modes around the bonds, which are far from the reaction mode of cycloaddition. The possibility of a c3 monoadduct is consistent with the regioselectivity observed at low temperatures using X-ray single-crystal diffraction,[13,14] as shown in the Supporting Information (Figure S2). It should be noted that thermal rotation of the La_2 molecule inside the adducts might be possible after the reactions. The observed structure is therefore not necessarily equal to the kinetic product. Our theoretical prediction is valid for predicting a kinetic product. In this case, the kinetic and final major products are found to be the same c3 adducts. The atomic VCCs (AVCCs),[27] i.e., atomic contributions to vibronic couplings, for the effective modes can be seen in the Supporting Information (Figure S8).

Figure 6 shows the VCCs for the localized stretching vibrations of the carbon bonds, which provide a quantitative

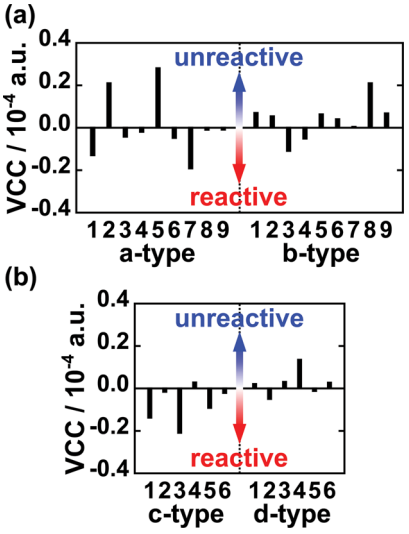

Figure 6. Vibronic coupling constants (VCCs) for localized stretching vibrations at different types of carbon bonds: (a) D_{2h} and (b) D_{3d} $La_2@C_{80}$ anion. a- and c-type bonds are [6,6] bonds, whereas b- and d-type bonds are [6,5] bonds (see definitions of bonds labeled in Figure 1). Bonds that have negative VCCs can be regarded as reactive sites. [6,6] bonds have smaller VCCs than [6,5] bonds. In particular, the c3 bonds have the smallest VCCs.

measure of bond reactivities. The sites that have negative VCCs will be stabilized by bond elongating vibrations and can therefore be regarded as reactive sites in cycloaddition. In contrast, the sites with positive values will be destabilized. As shown in Figure 6, the c3 bonds of the D_{3d} isomer are the most reactive. The figure also shows that a few [6,5] bonds such as the b3 bonds are slightly reactive and can yield minor products. This is consistent with experimental observations.[13,14]

We calculated energy barriers in the reaction between $La_2@C_{80}$ and *N*-methyl azomethine ylide, which is an electron donor. We chose the additions at three types of bonds, c3, c1, and a5 bonds. According to the VCD analysis, the reactivity order is c3 bond > c1 bond > a5 bond. It should be noted that the c1 bond has the largest distribution of LUMO density. The calculated energy barriers were 364 meV (c3 bond) < 483 meV (c1 bond) < 560 meV (a5 bond). This is consistent with the result of the VCD analysis. The computational details are described in the Supporting Information.

4.2. Electrophilic Attack on $La_2@C_{80}$. Figure 7 shows the electron density differences $\Delta\rho$ between the neutral $La_2@C_{80}$

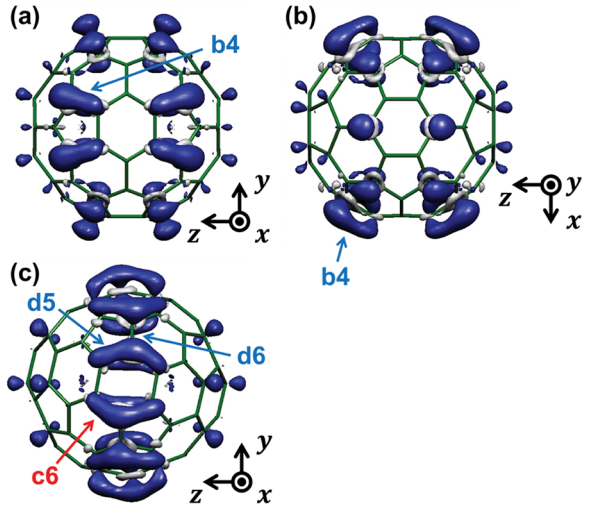

Figure 7. Electron density differences $\Delta\rho$ between neutral and cationic states of isolated $La_2@C_{80}$ isomers: (a, b) D_{2h} isomers from different perspectives and (c) D_{3d} isomer. Isosurface values are 5.0×10^{-4} a.u. Blue surfaces show negative regions (electron decrease), and gray surfaces show positive regions (electron increase). The b4 bonds have large $\Delta\rho$ distributions. From the vibronic coupling calculations, the b4, d5, and c6 bonds are the first, second, and third reactive sites, respectively (see Figure 11). The d6 bonds have small $\Delta\rho$ because the corresponding LUMO distributions are antibonding.

isomers and their cations. The $\Delta\rho$ for the $La_2@C_{80}$ cations is similar to the highest occupied molecular orbital (HOMO) densities with belt-like distributions on the C_{80} cages. Figures 8 and 9 show the effective modes *s* of the $La_2@C_{80}$ cations and the corresponding potential derivatives υ_s, respectively. Large positive distributions of υ_s can be seen on the b4, c6, and d5 bonds. As shown in Figure 7, these sites also have large $\Delta\rho$. In particular, the b4 bonds (a type of [6,5] bond) of the D_{2h}

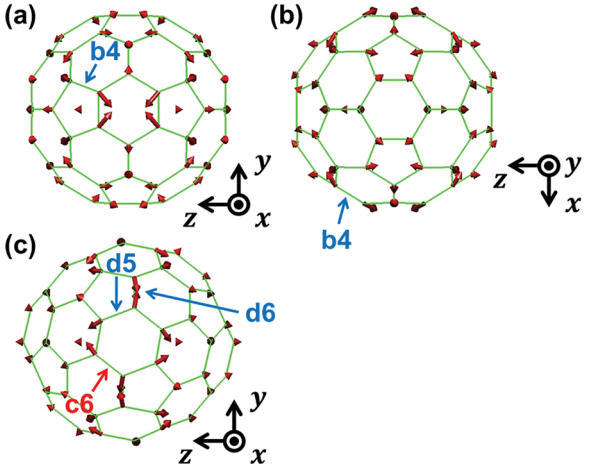

Figure 8. Effective vibrational vectors *s* of isolated $La_2@C_{80}$ cations: (a, b) D_{2h} isomers from different perspectives and (c) D_{3d} isomer. The b4, d5, and c6 bonds are elongated by the effective modes, whereas the d6 bonds are shortened.

dx.doi.org/10.1021/jo502208t | *J. Org. Chem.* 2015, 80, 141−147

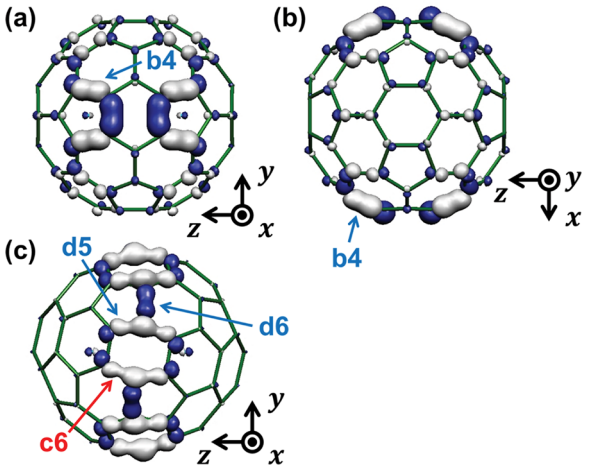

Figure 9. Potential derivatives υ_s for effective modes s of isolated $La_2@C_{80}$ cations: (a, b) D_{2h} isomers from different perspectives and (c) D_{3d} isomer. Isosurface values are 5.0×10^{-3} a.u. Blue surfaces show negative regions, and gray surfaces show positive regions. A large positive distribution on a bond indicates that the bond is easily elongated by the approach of an electrophile. The b4, d5, and c6 bonds have large positive υ_s, whereas the d6 bonds have negative distributions.

isomer not only have the largest $\Delta\rho$ distributions but also the largest υ_s distributions.

Figure 10 shows the η_s of $La_2@C_{80}$ cations for the effective modes and η_s of the ethylene anion for comparison. As shown

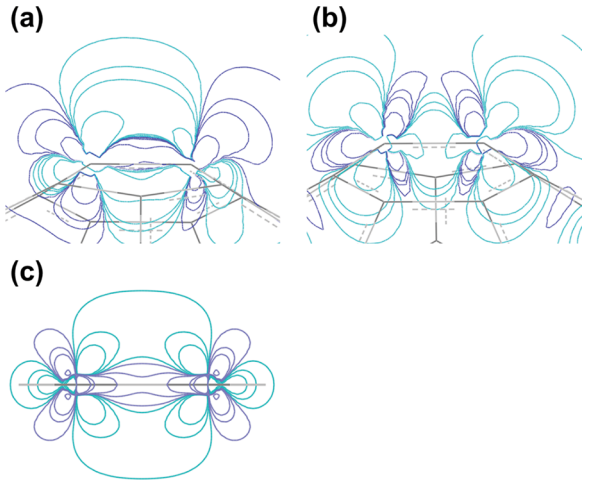

Figure 10. Vibronic coupling densities (VCDs) η_s of isolated $La_2@C_{80}$ cations for the effective modes: (a) b4 bond and (b) d6 bond. (c) η_s of ethylene cation for the effective mode. The VCD at the b4 bond, which has a large $\Delta\rho$, is similar to that of the ethylene cation. On the other hand, the VCD at the d6 bond is completely different from that of the ethylene cation.

in the figure, the b4 bond has the same η_s distribution as that of the ethylene cation. This indicates the existence of ethylene moieties as functional groups at the b4 bonds. In contrast to the b4 bonds, the d6 bonds have completely different η_s distributions from those of the ethylene cation; therefore, these are not reactive sites. The prediction of a b4 monoadduct is consistent with the reactive sites observed at low temperatures using X-ray single-crystal diffraction,[15] as shown in the Supporting Information (Figure S2). The observed structure is not necessarily the same as the kinetic product because of the thermal rotation of the La_2 molecule. In this case, the kinetic product (b4 adduct) is found to be the same as the final product. For electrophilic cycloadditions, the frontier orbital theory predicts the same regioselectivity as that from the VCD analysis (see the Supporting Information, Figure S5). The AVCCs for the effective modes are shown in the Supporting Information (Figure S9).

Figure 11 shows the VCCs at the localized stretching vibrations for all types of carbon bonds. As shown in Figure 11,

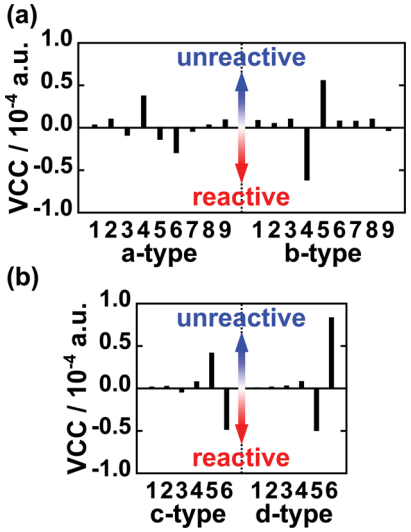

Figure 11. Vibronic coupling constants (VCCs) for localized stretching vibrations at different types of carbon bonds: (a) D_{2h} and (b) D_{3d} $La_2@C_{80}$ cation. a- and c-type bonds are [6,6] bonds, and b- and d-type bonds are [6,5] bonds (see definitions of bonds labeled in Figure 1). Bonds that have negative VCCs can be regarded as reactive sites. [6,5] bonds have smaller VCCs than [6,6] bonds. In particular, the b4 bonds have the smallest VCCs.

the [6,5] bonds such as the b4 and d5 bonds are found to be reactive. Particularly, the b4 bonds of the D_{2h} isomer are the most reactive. In addition, [6,6] bonds with negative VCCs such as the c6 bonds may yield minor products.

5. CONCLUSIONS

We theoretically clarified the regioselectivities of $La_2@C_{80}$ in nucleophilic and electrophilic attacks using vibronic coupling density analysis. The c3 bonds (a type of [6,6] bond) of the D_{3d} $La_2@C_{80}$ isomer were found to be the most reactive in nucleophilic attacks, consistent with experimental observations. Although the c3 bonds have small $\Delta\rho$ and LUMO densities, they have a large potential derivative with respect to a reaction mode. For nucleophilic cycloadditions, therefore, the degrees of freedom of nuclear motions are important.

In addition, the present theory predicted that the b4 bonds (a type of [6,5] bond) of the D_{2h} isomer are the most reactive in electrophilic attacks, which is also consistent with the experimental observations. The b4 bonds have large HOMO densities; thus, the frontier orbital theory, like the present theory, correctly predicts the regioselectivity for electrophilic attacks.

Recently, Garcia-Borràs et al. have theoretically investigated the Diels–Alder reaction between $La_2@C_{80}$ and butadiene.[21] According to their study, the energy barriers of the [6,6] and

dx.doi.org/10.1021/jo502208t | J. Org. Chem. 2015, 80, 141–147

[6,5] attacks are close to each other. This is because butadiene is not a strong nucleophile or electrophile. The net charge transfer between $La_2@C_{80}$ and butadiene is not so large. Accordingly, both of the charge transfers from $La_2@C_{80}$ to butadiene and from butadiene to $La_2@C_{80}$ should be almost equally taken into consideration. $\Delta\rho$ in this case is the mixture of $\Delta\rho$ for a nucleophilic attack and $\Delta\rho$ for an electrophilic attack. The VCD theory predicts that both of the [6,6] and [6,5] bonds are reactive. This is consistent in that the energy barriers of the [6,6] and [6,5] attacks in this reaction are close.

The VCDs illustrate the origin of the coupling between the electronic and vibrational states. On the other hand, the conventional reactivity indices such as frontier orbital density consider only the electronic state. The frontier orbital theory predicts a regioselectivity in terms of the stabilization due to the charge-transfer interaction between approaching reactants, depending on the approaching orientation. In the case of fullerenes, the charge-transfer interaction is almost the same for every orientation. Therefore, the frontier orbital theory fails to predict the reactivity of such fullerenes. $La_2@C_{80}$ is such a case. On the other hand, the vibronic couplings of the fullerenes depend on orientations. The vibronic coupling density analysis can predict the regioselectivity in terms of the stabilization due to vibronic couplings after the charge transfer, depending on the approaching orientation. The present study shows that the stabilization due to vibronic couplings plays an important role in the regioselectivity of nucleophilic cycloadditions to $La_2@C_{80}$.

A picture of the functional groups, which are the double bonds of ethylene moieties, could be extracted from the VCD with respect to the effective mode. The regioselectivity could be predicted using VCD analysis with respect to the localized modes.

■ ASSOCIATED CONTENT

Supporting Information

Schlegel diagram of $La_2@C_{80}$, experimentally observed reactive sites of $La_2@C_{80}$, derivation of vibronic coupling density (VCD), optimized geometries, bond energies, orbital levels, frontier orbitals, Mulliken charges, π-orbital axis vector (POAV) pyramidalization angles, atomic vibronic coupling constants (AVCCs) for the effective modes, and computational method of reaction barriers. This material is available free of charge via the Internet at http://pubs.acs.org.

■ AUTHOR INFORMATION

Corresponding Author

*E-mail: tsato@moleng.kyoto-u.ac.jp. Phone: (+81)-75-383-2803. Fax: (+81)-75-383-2555.

Notes

The authors declare no competing financial interest.

■ ACKNOWLEDGMENTS

Numerical calculations were partly performed at the Supercomputer Laboratory of Kyoto University and the Research Center for Computational Science in Okazaki, Japan.

■ REFERENCES

(1) Chaur, M.; Melin, F.; Ortiz, A.; Echegoyen, L. *Angew. Chem., Int. Ed.* **2009**, *48*, 7514−7538.

(2) Yamada, M.; Akasaka, T.; Nagase, S. *Acc. Chem. Res.* **2010**, *43*, 92−102.

(3) Lu, X.; Akasaka, T.; Nagase, S. *Chem. Commun.* **2011**, *47*, 5942−5957.

(4) Osuna, S.; Swart, M.; Solà, M. *Phys. Chem. Chem. Phys.* **2011**, *13*, 3585−3603.

(5) Zhang, J.; Stevenson, S.; Dorn, H. C. *Acc. Chem. Res.* **2013**, *46*, 1548−1557.

(6) Popov, A. A.; Yang, S.; Dunsch, L. *Chem. Rev.* **2013**, *113*, 5989−6113.

(7) Heath, J. R.; O'Brien, S. C.; Zhang, Q.; Liu, Y.; Curl, R. F.; Tittel, F. K.; Smalley, R. E. *J. Am. Chem. Soc.* **1985**, *107*, 7779−7780.

(8) Kobayashi, S.; Mori, S.; Iida, S.; Ando, H.; Takenobu, T.; Taguchi, Y.; Fujiwara, A.; Taninaka, A.; Shinohara, H.; Iwasa, Y. *J. Am. Chem. Soc.* **2003**, *125*, 8116−8117.

(9) Ross, R. B.; Cardona, C. M.; Guldi, D. M.; Sankaranarayanan, S. G.; Reese, M. O.; Kopidakis, N.; Peet, J.; Walker, B.; Bazan, G. C.; Keuren, E. V.; Holloway, B. C.; Drees, M. *Nat. Mater.* **2009**, *8*, 208−212.

(10) Cagle, D. W.; Kennel, S. J.; Mirzadeh, S.; Alford, J. M.; Wilson, L. J. *Proc. Natl. Acad. Sci. U.S.A.* **1999**, *96*, 5182−5187.

(11) Shimotani, H.; Ito, T.; Iwasa, Y.; Taninaka, A.; Shinohara, H.; Nishibori, E.; Takata, M.; Sakata, M. *J. Am. Chem. Soc.* **2004**, *126*, 364−369.

(12) Zhang, J.; Hao, C.; Li, S.; Mi, W.; Jin, P. *J. Phys. Chem. C* **2007**, *111*, 7862−7867.

(13) Yamada, M.; Wakahara, T.; Nakahodo, T.; Tsuchiya, T.; Maeda, Y.; Akasaka, T.; Yoza, K.; Horn, E.; Mizorogi, N.; Nagase, S. *J. Am. Chem. Soc.* **2006**, *128*, 1402−1403.

(14) Yamada, M.; Okamura, M.; Sato, S.; Someya, C.; Mizorogi, N.; Tsuchiya, T.; Akasaka, T.; Kato, T.; Nagase, S. *Chem.—Eur. J.* **2009**, *15*, 10533−10542.

(15) Yamada, M.; Minowa, M.; Sato, S.; Slanina, Z.; Tsuchiya, T.; Maeda, Y.; Nagase, S.; Akasaka, T. *J. Am. Chem. Soc.* **2011**, *133*, 3796−3799.

(16) Takano, Y.; Obuchi, S.; Mizorogi, N.; García, R.; Herranz, M. A.; Rudolf, M.; Guldi, D. M.; Martín, N.; Nagase, S.; Akasaka, T. *J. Am. Chem. Soc.* **2012**, *134*, 19401−19408.

(17) Yamada, M.; Someya, C.; Wakahara, T.; Tsuchiya, T.; Maeda, Y.; Akasaka, T.; Yoza, K.; Horn, E.; Liu, M. T. H.; Mizorogi, N.; Nagase, S. *J. Am. Chem. Soc.* **2008**, *130*, 1171−1176.

(18) Ishitsuka, M. O.; Sano, S.; Enoki, H.; Sato, S.; Nikawa, H.; Tsuchiya, T.; Slanina, Z.; Mizorogi, N.; Liu, M. T. H.; Akasaka, T.; Nagase, S. *J. Am. Chem. Soc.* **2011**, *133*, 7128−7134.

(19) Feng, L.; Radhakrishnan, S. G.; Mizorogi, N.; Slanina, Z.; Nikawa, H.; Tsuchiya, T.; Akasaka, T.; Nagase, S.; Martín, N.; Guldi, D. M. *J. Am. Chem. Soc.* **2011**, *133*, 7608−7618.

(20) Yamada, M.; Someya, C. I.; Nakahodo, T.; Maeda, Y.; Tsuchiya, T.; Akasaka, T. *Molecules* **2011**, *16*, 9495−9504.

(21) Garcia-Borràs, M.; Osuna, S.; Luis, J. M.; Swart, M.; Solà, M. *Chem.—Eur. J.* **2013**, *19*, 14931−14940.

(22) Fukui, K.; Yonezawa, T.; Shingu, H. *J. Chem. Phys.* **1952**, *20*, 722−725.

(23) Fukui, K. *Acc. Chem. Res.* **1971**, *4*, 57−64.

(24) Mulliken, R. S. *J. Chem. Phys.* **1955**, *23*, 1833−1840.

(25) Haddon, R. C. *Science* **1993**, *261*, 1545−1550.

(26) Sato, T.; Tokunaga, K.; Tanaka, K. *J. Phys. Chem. A* **2008**, *112*, 758−767.

(27) Sato, T.; Tokunaga, K.; Iwahara, N.; Shizu, K.; Tanaka, K. In *The Jahn−Teller Effect: Fundamentals and Implications for Physics and Chemistry*; Köppel, H., Yarkony, D. R., Barentzen, H., Eds.; Springer Series in Chemical Physics; Springer-Verlag: Berlin, 2009; Vol. *97*, pp 99−129.

(28) Sato, T.; Iwahara, N.; Haruta, N.; Tanaka, K. *Chem. Phys. Lett.* **2012**, *531*, 257−260.

(29) Haruta, N.; Sato, T.; Iwahara, N.; Tanaka, K. *J. Phys.: Conf. Ser.* **2013**, *428*, 012003.

(30) Haruta, N.; Sato, T.; Tanaka, K. *Tetrahedron* **2014**, *70*, 3510−3513.

(31) Haruta, N.; Sato, T.; Tanaka, K. *J. Org. Chem.* **2012**, *77*, 9702−9706.

(32) Sato, T.; Uejima, M.; Iwahara, N.; Haruta, N.; Shizu, K.; Tanaka, K. *J. Phys.: Conf. Ser.* **2013**, *428*, 012010.
(33) Haruta, N.; Sato, T.; Tanaka, K.; Baron, M. *Tetrahedron Lett.* **2013**, *54*, 5920−5923.
(34) Parr, R. G.; Yang, W. *J. Am. Chem. Soc.* **1984**, *106*, 4049−4050.
(35) Hellmann, H. *Einführung in die Quantenchemie*; Deuticke and Company: Leipzig, 1937.
(36) Feynman, R. P. *Phys. Rev.* **1939**, *56*, 340−343.
(37) Vosko, S. H.; Wilk, L.; Nusair, M. *Can. J. Phys.* **1980**, *58*, 1200−1211.
(38) Becke, A. D. *Phys. Rev. A* **1988**, *38*, 3098−3100.
(39) Perdew, J. P. *Phys. Rev. B* **1986**, *33*, 8822−8824.
(40) van Lenthe, E.; Baerends, E. J. *J. Comput. Chem.* **2003**, *24*, 1142−1156.
(41) van Lenthe, E.; Baerends, E. J.; Snijders, J. G. *J. Chem. Phys.* **1993**, *99*, 4597−4610.
(42) te Velde, G.; Bickelhaupt, F. M.; Baerends, E. J.; Guerra, C. F.; van Gisbergen, S. J. A.; Snijders, J. G.; Ziegler, T. *J. Comput. Chem.* **2001**, *22*, 931−967.
(43) Guerra, C. F.; Snijders, J. G.; te Velde, G.; Baerends, E. J. *Theor. Chem. Acc.* **1998**, *99*, 391−403.
(44) *ADF2012*; SCM: Amsterdam, The Netherlands; http://www.scm.com.